CHAPTER 4

EXPERIMENTAL SETUP AND PROCEDURE

4.1 Introduction

This chapter explains the experimental facilities and testing procedure which are adopted for acquiring experimental data. The experimental facility is a two-phase flow test rig which is developed in the laboratory of Instrumentation and Control in the department of Electrical and Electronic Engineering of Universiti Teknologi PETRONAS. The experimental setup is elaborated by using facility pictures along with P&ID. The operating conditions, data acquisition system and experimental procedure are also discussed in detail.

4.2 Two-Phase Flow Test Setup

The experimental setup was designed to continuously process the two-phase fluid with different operating conditions in real time. This setup is basically a test rig consists of two main sections namely:

i. Metering section

ii. Test section

The metering section consists of the fluid supply measurement and control system which is capable of supplying air and deionised water at various controlled flow rates. The test section consists of an ECT sensor (i.e. co-current bubble column), control valves and differential pressure transducer. Each of this flow section is equipped with the suitable instrumentation to ensure correct measurement of fluid flow rate, pressure and temperature. The details are provided in later sections. A schematic of an experimental test rig is shown in Figure 4.1.

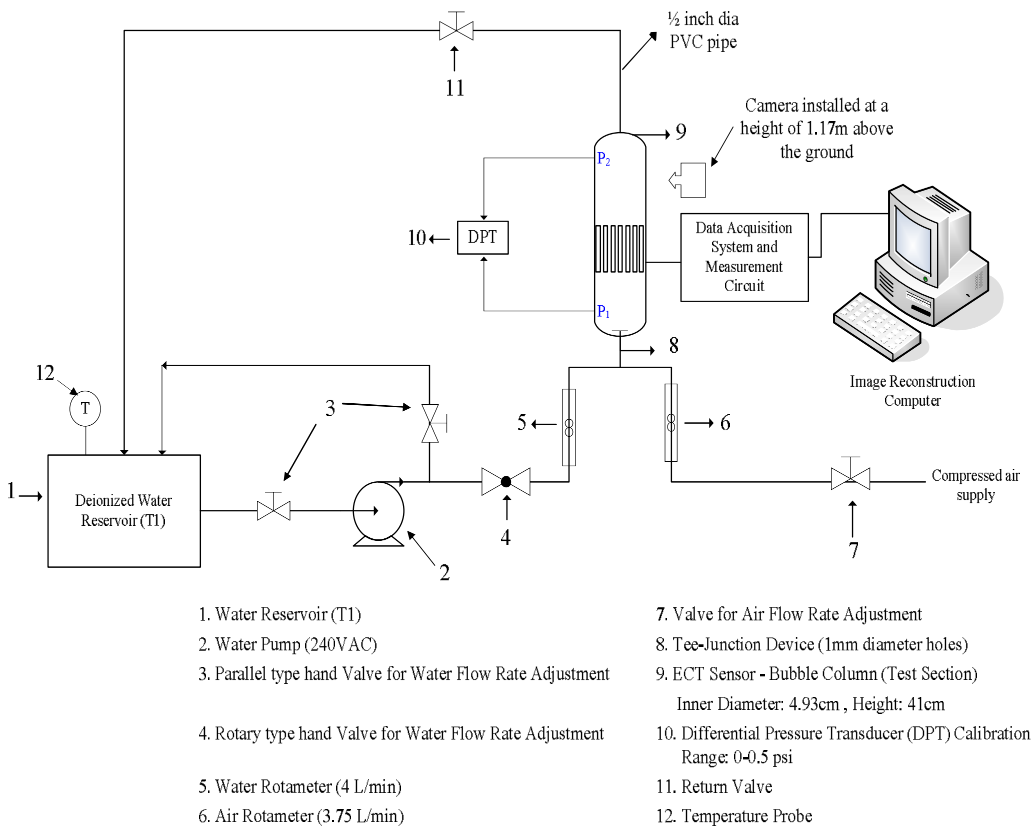

Figure 4.1: Schematic of an Experimental Setup.

4.3 Test Fluid

The fluid used in the loop for test is compressed air and deionised water. This section describes the fluids conditions and their use. The physical properties of the air and deionised water are mentioned in Table 4.1.

Table 4.1: Physical Properties of Air and Deionised Water Used in the Experiment

	μ (Ns/m^2)	**ρ (kg/m^3)**	**σ (μS/cm)**
Air	1.85 X 10^{-5}	1.204	-
Deionised Water	1.002 X 10^{-3}	998.2	0.35

a) *Test Gas*

The gas used in the test rig is compressed air. The air is compressed before it is delivered into the experimental loop.

b) *Deionised Water*

The water used in the rig is deionised water. The deionized water is obtained from a Purelab Option Water Purification System which produces water with a resistivity of 18 Mega Ohm-cm. The density of the water is about 998.2 kg/m^3 at 20 °C. The deionised water is stored in a covered water storage tank of capacity about 100 litres.

4.4 Fluid Supply Facilities

The fluid supply facilities are divided into two parts and are discussed below:

i. *Gas supply - atmospheric air*

The compressed air is supply from the University air compressor services. It supplies air normally at 0.4 to 0.6 MPa pressure.

ii. Liquid supply - deionised water

The deionised water is stored in a covered tank. The tank T1 is of 100 L capacity. It is supplied by a self priming electro pump (EBARA, JESXM5), as indicated in Figure 4.1 at position number 2, water pump (240VAC). The water is pumped into the metering section where the flow rate is being measured. The specifications of a water supply pump are mentioned in Table 4.2.

Table 4.2: Specifications of Water Pump

Parameters	**Measurement**
Type of Liquid	Clean Water
Max. Temperature	45 $^{\circ}$C
Max. Working Pressure	0.6 MPa
Type of Motor	Single Phase
Power Rating	0.37 kW/ 0.5 HP
Voltage	230 - 240 V
Capacity	0.5 - 45 L/min

4.5 Metering Section

The measurement of the flow rate and other conditions of fluid used in the experiment is provided by the metering facilities installed at the test rig. The fluid supply from the supply facility is measured and monitored by various measuring instruments. The measurement of the liquid flow rate is accomplished by using a Polysulfone flow meter (Model no. 6B0100-02D); labelled in Figure 4.1 as legend No. 5, water rotameter (4L/min). It has a range from 0.5 to 4 L/min corresponding to U_{sl} of 0.00436 to 0.034 m/sec. Figure 4.2 (a) gives the physical representation of the water rotameter while the detailed specifications of the rotameter can be found in Appendix ‘*B*’.

A separate flow meter is installed for the air flow rate measurement as mentioned in Figure 4.1 by legend No. 6, air rotameter (3.75 L/min). The air flow meter used in the rig is named as Acrylic flow meter (Model no. 6A0105BN-AB) with 1/8” brass fittings. The operating range of air rotameter is from 0.25 to 3.75 L/min corresponding to U_{sg} of 0.00218 to 0.0305 m/sec. Figure 4.2 (b) shows the front view of air rotameter. Further details on the specifications can be seen in Appendix ‘*C*’.

(a) (b)

Figure 4.2: Rotameters (a) Polysulfone-Water and (b) Acrylic-Air.

4.6 Test Section

The test section consists of an Electrical Capacitance Tomography (ECT) sensor (0.41 m in length) installed vertically on the test rig. The height of the test rig is about 1.5 m. The detailed specification of the sensor is mentioned in Table 4.3. The test section (i.e. ECT sensor) is made up of Perspex material which helps in visualisation of an air-water flow entering the column. The column is connected with inlet and outlet ½” diameter PVC piping network to allow dynamic flow of air and deionised water. The ECT sensor consists of a ring of 12-electrodes (which are separated from each other by small gap) on its outer periphery. It is connected with the data acquisition system which is then connected with a control computer by the built-in ECT software as mentioned in Figure 4.3. There are two types of control valves i.e. (parallel type and rotary type) that are also installed on the test rig for the adjustment of air and water flow rates.

Table 4.3: ECT Sensor Specifications

Parameters	Measurement
Number of electrodes	12
Material	Perspex
Inner diameter of pipe	49.3 mm
Outer diameter of pipe	65.2 mm
Outlay Screen diameter	120 mm
Thickness	8 mm
Length of sensor	410 mm
Length of electrodes	100 mm
Width of electrodes	22 mm
Thickness of electrodes	1 mm

Figure 4.3: ECT Sensor Connected with Data Acquisition Unit.

The test rig was also equipped with a differential pressure transmitter for flow measurements. The Smar - LD301 intelligent differential pressure transmitter is installed between the two ports named as P_1 (inlet point) and P_2 (outlet point) on the column to get the Delta-P measurements as shown in Figure 4.4.

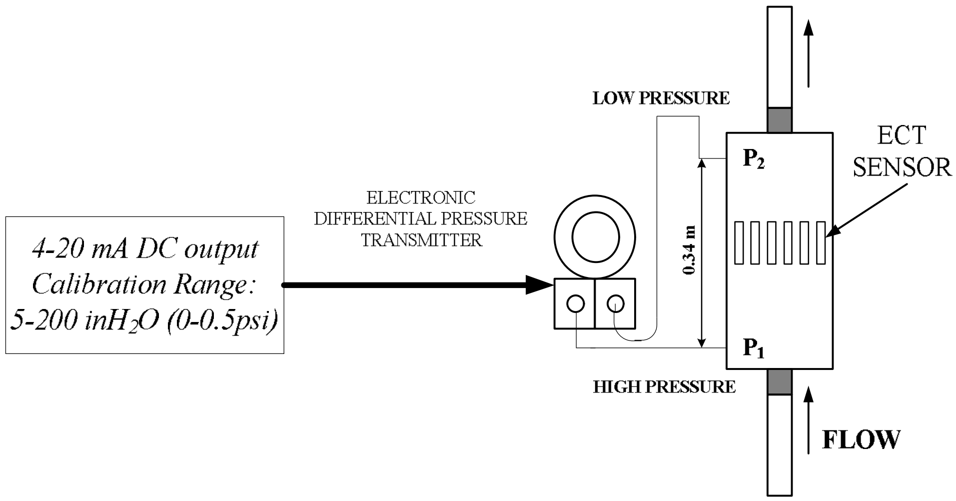

Figure 4.4: Position Mentioned for the Installation of Differential Pressure Transmitter.

4.7 Bubbles Generation

In order to generate the bubble flow regime several efforts have been done to get uniform sized bubbles. A multiple-orifice equally spaced nozzle has been installed at the bottom of the column with total seven (1 mm diameter each) holes on its surface to generate uniform bubbles. Figure 4.5 shows the top view of multiple orifice nozzle.

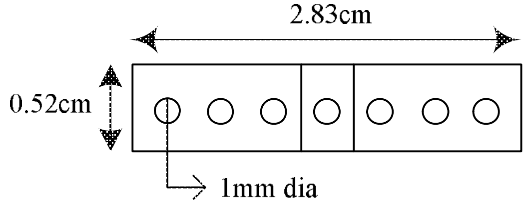

Figure 4.5: Multiple Orifice Nozzle for Bubbles Generation (Top view).

4.8 Instrumentation

This section outlines the details of the instrumentation used to carry out the experimental work. All the instruments along with their ranges and uncertainty are summarised in Table 4.4.

Table 4.4: Instrumentation Ranges and Accuracy

Signal Type	Manufacturer/ Model No.	Range	Accuracy
Volumetric flow rate: Water	Dakota Instruments, USA / Polysulfone 6B0100-02D (1/2" MNPT Adapter size)	0.4-4.0 LPM, 0.1-1.0 GPM	± 5%
Volumetric flow rate: Air	Dakota Instruments, USA / ACR-Acrylic 6A0105BN-AB (1/8" FNPT Adapter size)	3.5 LPM / 7.0 SCFH	± 5%
Differential Pressure Transducer	SMAR-LD301	5 to 200 in H2O	± 0.075%
Temperature Probes	Foxboro I/A series Intelligent Temperature Transmitter/ Model RTT20-T1WRKFN-L1	- 40 to 750 °C	For 4 to 20 mA output accuracy, add ± 0.05% of span to digital accuracy
Video Images and Movies	DSC-HX1	230,000 pixels	-

4.8.1 Rotameter

The air and deionised water volumetric flow rates were measured by two different rotameters. The deionised water (with conductivity continuously measured according to the temperature) is supplied from a pump and regulated by a bypass line and the control valves. Air is pumped via compressed line through a rotameter and enters the sensor from the bottom through T-junction multiple orifice nozzle to generate the bubbles after mixing with water. The test loop can supply up to 3 LPM of air and 4 LPM of deionised water at room temperature. The deionised water from the main column flowed upward together with air from the upper part of an ECT sensor and returns to a separate reservoir through a 0.0127 m diameter PVC pipe.

4.8.2 Differential Pressure Transducer

The differential pressure transducer is installed in the vertically oriented Perspex column at two different ports i.e. P_1 and P_2 as mentioned in the above figures 4.1 and 4.5 respectively. The placement of the differential pressure transducer in the Perspex column allowed visual observations of the flow pattern along with the measured differential pressure. The transducer is placed at approximately 1.2 m from the ground level. The differential pressure transducer is ranged from 5 to 200 in H_2O with 0.075% accuracy (specifications mentioned in Appendix '*D*'). The regular flushing from the tappings was performed before each run to prevent the ingress of air and hence affecting the hydrostatic head. Later, these readings of differential pressure were used to calculate the void fraction.

4.8.3 Temperature Probes

The temperature of the working fluid (i.e. air and water) was also monitored before entering into the vertical test section. The temperature of the incoming air and water into the column was measured by Foxboro I/A series temperature transmitter model RTT20 having range of -40 to 750 °C and for 4 to 20 mA output accuracy, add ± 0.05% of span to digital accuracy.

4.9 Data Acquisition System

The details to acquire the data from the data acquisition system and its software used in this experimental setup are discussed below.

4.9.1 ECT System Overview

The ECT data acquisition system used in this study has been developed to do online monitoring of multiphase flows by providing detailed information such as multiphase flow pattern, flow regime and velocity. The ECT module produces permittivity maps from multi-electrode sensors arranged around the pipe. ECT performs three main operations:

i. Calibration of a Sensor

ii. Data Acquisition

iii. Data Processing

Initially the software calibrates the sensor with materials of low and high permittivity and further analyzed the data in the form of raw and image analysis on other software. The ECT sensor consists of an array of electrodes attached to the periphery of the vessel which is to be imaged. It is a common practice to calibrate an ECT sensor using two different materials for example, air and deionized water. They have different dielectric properties, particularly the permittivity value. An ECT system is calibrated one for lower permittivity limit and another for the higher permittivity limit. In this case, the sensor is first measured empty i.e. using air having the permittivity equals to one, and then it is completely filled with deionized water having the higher permittivity equals to 80. The physical layout of the sensor with shield and without shield is shown in Figure 4.6 (a) and (b) respectively.

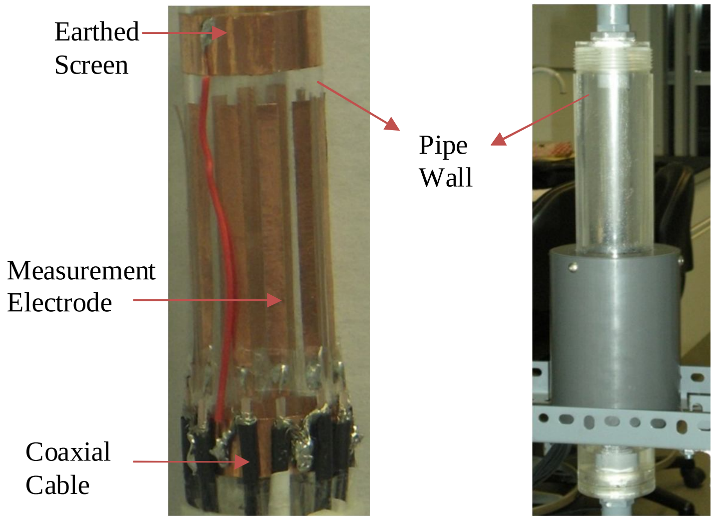

(a) Sensor without Shield

(b) Sensor with Shield

Figure 4.6: 12-Electrode ECT Sensor.

The available ECT system in the laboratory can be used for 8, 12 or 16 number of electrodes connecting on Plane 1 or Plane 2 respectively. The encoded tomographic process data to the computer is routed from each sub-system via a high-speed serial data link to USB port mounted in the PC. Each acquisition sub-system in the data acquisition unit is controlled by a Processing and Communication Card (PCC), which supports the communication link to the PC and also provides test control and Digital Signal Processing (DSP) for data pre-processing. The front panel connectors allow the data acquisition unit to be connected to the tomographic sensors [83]. The detailed specification of the data acquisition system is given in Appendix '*E*'.

The acquisition system is connected with a PC for data storage, processing and display. The minimum requirements for the PC is equipped with Pentium IV (or later) processor with a minimum of 256 MB of system memory and typically 50 GB of disk storage. The display unit have minimum resolution of 800 x 600 pixels and the windows operating package is Microsoft XP.

4.9.2 ECT Software

The ECT software is based on visual programming paradigm and designed for controlling and measuring process data online from the process tomography system. The software allows visualizing multi-components system such as air/water in real time. A single graphic user interface (GUI), the *Configurator*, provides control of the system and selection of post-processing and reconstruction tasks. Hence, it is able to define and configure the modules that are needed to interact either during an online experiment, or offline post-processing of data. Each module will have one or more of the following elements [83]:

i. Input – is required to perform a particular operation that the module is designed for

ii. Output – is produced as a result of the operation by the module and may be used by others

iii. Parameters – is used to control how the operation is performed

iv. Description – is used to tell others how the module should be use.

A pre-defined flow as shown in Figure 4.7 is used for controlling the online measurements. This flow analyze using one plane; 12-electrodes per plane. Its functions include online measurement, display and save. The settings in each step are as follows:

i. Protocol - Number of electrodes, current inject base, voltage inject base and array size

ii. Calibration - Low / High calibration, measurement

iii. Acquisition - Pipe width, min and max permittivity, number to average and time interval

iv. Others - Location of storing the data.

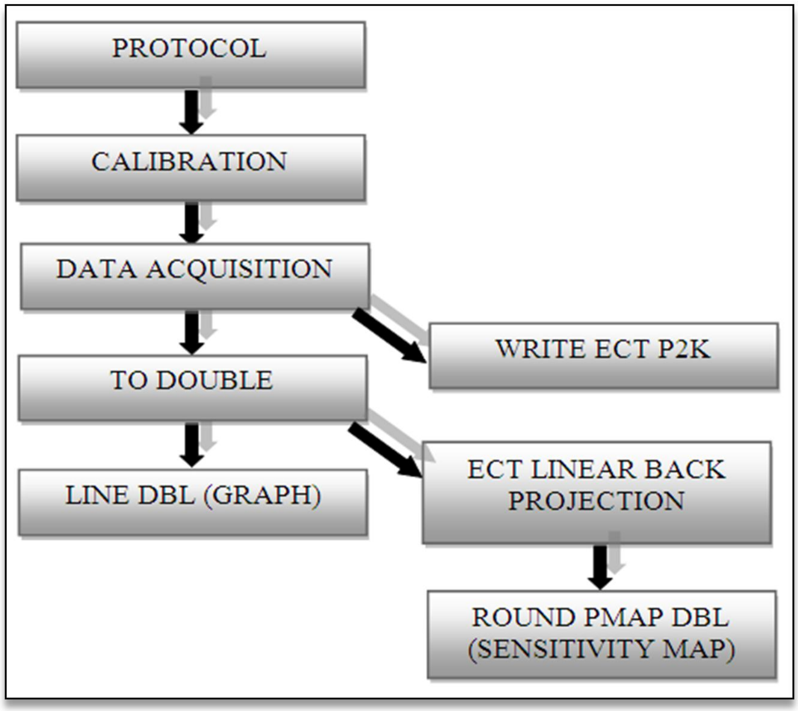

Figure 4.7: ECT Predefined Flow.

The basic steps that are required to get the measurement data from the online measurements of acquisition system for 12-electrode ECT sensor are discussed below. This will lead to extract the data for further measurement and analysis.

i. Connect ECT sensor cables to the 'ctp1' 1-8 electrodes and 'ctp1*' to 9-12 electrodes

ii. Connect power adapter lead to the data acquisition system

iii. Switch the front panel 'Grey' button – red light

iv. Switch ECT power on from the back panel – light blinking on *cdsp* board

v. Open the MMTC Configurator

vi. Open the file Ect-onep-1.tsc

vii. Fully filled the senor with air and set the 'ECT Cal' to low-'0'- Press 'Run'

viii. Fully filled the senor with deionised water and set the ‘ECT Cal’ to high-‘1’- Press ‘Run’

ix. For online measurement set ‘ECT Cal’ to none-‘2’- Press ‘Run’, it will generate number of frames.

4.9.3 Principle of Operation of ECT

The ECT system produces one or more cross-sectional images of the permittivity contents of a vessel or pipe from measurements of capacitance between different combinations of sensor electrodes which surround the vessel. The images are approximate and of relatively low resolution. Images are produced in the following ways:

i. The properties of the sensor are measured or calculated initially to produce a sensitivity map of the sensor.

ii. The sensor is normally calibrated at each end of the range of permittivities to be measured by filling the sensor with the lower permittivity material initially and measuring all of the individual inter-electrode capacitances. This is repeated using the higher permittivity material. The data obtained during the calibration procedure is used to set up the measurement parameters and stored in a calibration data file.

iii. Once the system has been calibrated, the capacitances between all unique pairs of sensor electrodes are measured continuously at high speed, giving N (N-1)/2 unique values per measurement.

iv. An image reconstruction algorithm is used to compute the cross sectional distribution of the permittivity of the material inside the pipe. Images can be constructed from the capacitance measurements either at the time of measurement (online) or from stored or captured data (offline).

v. The algorithm supplied as standard in the acquisition system is the so-called linear back-projection (LBP) algorithm. It is fast but approximate algorithm which uses the capacitance measurements, together with the sensitivity map to produce the image.

4.9.4 Capacitance Measurement Sequence

The ECT acquisition system is used to measure capacitances under *protocol 1* which has been discussed in section *3.2.1*. This means that one measurement electrode in each electrode plane and the equivalent driven guard electrode are set to be as 'source' electrodes, while the remaining (detector) electrodes are maintained at virtual earth potentials. This results in the arrangement of unique capacitance measurements for a 12-electrode sensor sequence as shown in Table 4.5.

Table 4.5: Measurement Set

Current Injection Points		Voltage Measurement Points										
		02	**03**	**04**	**05**	**06**	**07**	**08**	**09**	**10**	**11**	**12**
	01	C_{1-2}	C_{1-3}	C_{1-4}	C_{1-5}	C_{1-6}	C_{1-7}	C_{1-8}	C_{1-9}	C_{1-10}	C_{1-11}	C_{1-12}
	02		C_{2-3}	C_{2-4}	C_{2-5}	C_{2-6}	C_{2-7}	C_{2-8}	C_{2-9}	C_{2-10}	C_{2-11}	C_{2-12}
	03			C_{3-4}	C_{3-5}	C_{3-6}	C_{3-7}	C_{3-8}	C_{3-9}	C_{3-10}	C_{3-11}	C_{3-12}
	04				C_{4-5}	C_{4-6}	C_{4-7}	C_{4-8}	C_{4-9}	C_{4-10}	C_{4-11}	C_{4-12}
	05					C_{5-6}	C_{5-7}	C_{5-8}	C_{5-9}	C_{5-10}	C_{5-11}	C_{5-12}
	06						C_{6-7}	C_{6-8}	C_{6-9}	C_{6-10}	C_{6-11}	C_{6-12}
	07							C_{7-8}	C_{7-9}	C_{7-10}	C_{7-11}	C_{7-12}
	08								C_{8-9}	C_{8-10}	C_{8-11}	C_{8-12}
	09									C_{9-10}	C_{9-11}	C_{9-12}
	10										C_{10-11}	C_{10-12}
	11											C_{11-12}

Note: C_{1-2} means the capacitance measured between electrodes 1 and 2 with electrode 1 is used as a source electrode and electrode 2 set as a detector electrode.

4.9.5 Calibration Principle

An ECT system is normally calibrated by measuring two reference materials which in turn measure the resultant inter-electrode capacitance values at two extreme values of relative permittivity. It is calibrated with a lower permittivity material, followed by a higher permittivity material, in order to obtain the full range of variation in the measured capacitance. For the experimental study undertaken, the sensor was calibrated with air as a low permittivity material and deionised water as a high permittivity material. When a high permittivity object is introduced into a low permittivity background in the imaging area (i.e. inside the sensor), the capacitances of electrode pairs will change. An ECT system measures these capacitance changes and reconstructs a cross-sectional image from the measured data [70].

4.9.6 Normalisation of Inter-electrode Capacitances

Normalisation has been defined in the section *3.2.4.1*. For the current study, the sensor is first measured empty to obtain the lower capacitance C_l and then it is completely filled with deionised water to obtain the higher capacitance C_h. The measured capacitance C_m can then be normalised by [69]:

$$C_n = \frac{C_m - C_l}{C_h - C_l} \tag{4-1}$$

where, C_n is the set of normalised inter-electrode capacitances.

4.10 Operating Conditions

All the measurements for void fraction and bubbles characteristics were carried out for air-water system at a temperature of approximately 20 ± 2 °C. The pressure at the compressed line was maintained at 0.4 to 0.6 MPa. The superficial gas velocity was varied between 0.0021 to 0.03 m/sec, and the superficial liquid velocity varied between 0.00425 to 0.034 m/sec.

4.11 Experimental Procedure

This section describes the working procedure designed to perform the series of experiments as follows:

i. At the start of each experimental run, the electrical connections from the sensors to the data acquisition unit were checked along with the inspection of pressure tappings and temperature probes.

ii. After performing the checks, air is pumped via compressed line through a rotameter and enters the sensor from the bottom.
iii. The deionised water (with conductivity continuously measured according to the temperature) is supplied from a pump and is regulated by a bypass line and the hand valve. The deionised water flows into the bottom part of an ECT sensor (i.e. co-current bubble column) and mixed with the compressed air before entering into the test section of the sensor.
iv. The air and deionised water flow is controlled by means of air and water rotameters respectively.
v. The air-water mixture flows out from the upper part of the column and returns to a separate water reservoir through a ½” diameter PVC pipe.
vi. A series of experiments were performed on the test rig by using online calibration procedure. During these experiments, the ECT sensor was connected with the piping loop by using connectors.
vii. The test section was initially pressurised with air, followed by deionised water by opening the parallel and rotary hand valves.
viii. The differential pressure of the system was noted by using differential pressure transducer installed at the system.
ix. As a result of these experiments, different kinds of bubble flow regimes were identified and tested by varying the flow rates of air and deionised water accordingly.

4.11.1 Simulation Steps for an ECT Sensor

Kjell and Saba (2006) describe the procedures to model the electrical sensors using the Electromagnetic Module (EM) in COMSOL Multiphysics [58]. The modelling approach used can be listed as:

i. Choosing the electrostatics mode in the EM module.

ii. Drawing the sensor geometries. Sensor geometry is drawn using Graphical User Interface (GUI). The sensor consists of 12 electrodes and each electrode is mounted on 30° of the external diameter of the pipe. It is essential in this kind of sensor design to define sensor geometry as indicated in Figure 4.8 (a).

iii. Set electrical properties in the domains. Specify every material's properties. In this case, permittivities of every material should be specified. ε_{air} = 1.0, ε_{water} = 80.0, ε_{pw} = 3. Where ε_{air}, ε_{water} and ε_{pw} are the permittivities of air, water and pipe wall respectively as indicated in Figure 4.8 (b).

iv. Set the boundary conditions. The potential boundary conditions were applied to the sensor plates (electrodes). For one electrode, the boundary condition of *electric potential* ($V = V_0 = 15V$) was applied and all the remaining electrodes were kept at *ground potential* i.e. ($V = V_0 = 0V$). To represent the natural propagation of electric field, the default boundary condition of *continuity* ($n.(D_1-D_2) = 0$) was maintained for the internal boundaries. Figure 4.8 (c) shows the arrangement of each boundary condition when the first electrode was initialized. Grounded boundary (Green), initialized boundary/electric potential with 15V (Red), continuity boundary (Blue) and electric potential with 0V (Black).

v. Generating the mesh. According to finite element analysis, we have carry out imaging of regional triangulation, it is necessary to divide pixel pipelines into triangular finite element. Figure 4.8 (d) shows the corresponding nodes of triangular element mesh. Imaging region (i.e. the cross-sectional area of the pipeline of two-phase flow) was divided into 944 (coarse mesh) triangular elements while the optimum mesh element were used was 3768 (refine mesh). In order to achieve the higher accuracy the triangular mesh was used than quadrilateral.

vi. Solve and find the field distribution.

vii. Use the post-processing capabilities in COMSOL to compute the capacitance.

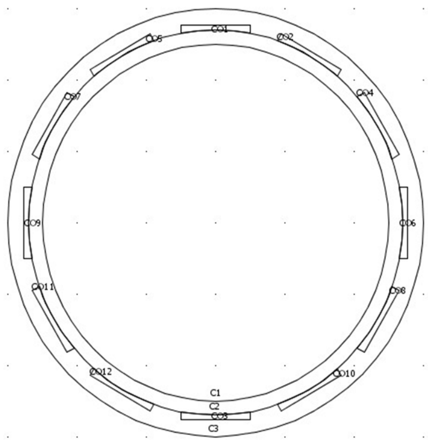

(a) Geometry Drawing

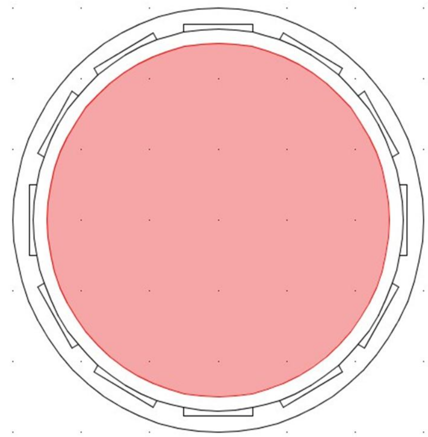

(b) Subdomain Settings

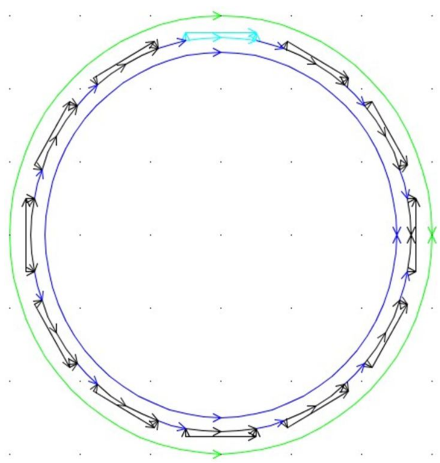

(c) Boundary Settings

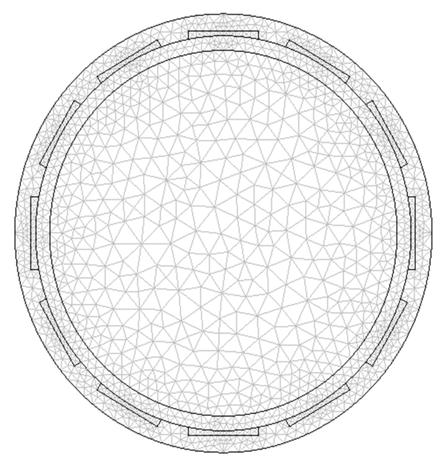

(d) 2D Finite Element Mesh

Figure 4.8: Simulation of Electrical Capacitance Sensor Model by COMSOL Software.

4.11.2 Test Matrix for Bubble Flow Regime

A series of tests were performed with different configurations as mentioned in the section *4.11*. The results obtained by varying the flow rates of air and deionised water are summarised in Table 4.6.

Table 4.6 shows the test case number, the differential pressure in psi, the air and water flow rates (Q_g and Q_w) in cubic metres per second, the air and water superficial velocities (U_{sg} and U_{sl}) in metres per second, and the different kinds of bubble flow regime observed from real time and ECT images that will be shown in next chapter. The superficial gas or liquid velocities used in Table 4.6 can be related to volumetric flow rate and cross-sectional area of the column is obtained from the below mentioned equations (4-2) and (4-3):

$$U_{sl} = \frac{Q_w}{A} \tag{4-2}$$

$$U_{sg} = \frac{Q_g}{A} \tag{4-3}$$

where,

$$A = \frac{D_i^2 \pi}{4} \tag{4-4}$$

On the variation in flow rates of air and water, different kinds of bubble flow regime being observed (as mentioned in Table 4.6) are as follows:

i. Discrete bubble flow

ii. Dispersed bubble flow and

iii. Coalesced bubble flow (They are explained in detail below).

Table 4.6: Test Matrix and Bubble Flow Regimes

Case No.	ΔP (psi)	Q_g x 10^{-5} (m^3/sec)	Q_w x 10^{-5} (m^3/sec)	U_{sg} x 10^{-3} (m/sec)	U_{sl} x 10^{-3} (m/sec)	Regime
1	0.445	0	1.67	0	8.74	Full of water
2	0.460	0	3.33	0	17.4	Full of water
3	0.485	0	5.00	0	26.2	Full of water
4	0.487	1.67	1.67	8.74	8.74	Discrete bubble flow
5	0.492	2.08	2.50	10.9	13.1	Discrete bubble flow
6	0.533	2.50	3.33	13.1	17.43	Discrete bubble flow
7	0.538	2.92	4.167	15.3	21.8	Dispersed bubble flow
8	0.543	3.33	5.00	17.43	26.2	Dispersed bubble flow
9	0.548	3.75	6.67	19.63	34.92	Dispersed bubble flow
10	0.513	4.167	1.67	21.8	8.74	Coalesced bubble flow
11	0.532	5.00	2.50	26.2	13.1	Coalesced bubble flow
12	0.55	5.83	3.33	30.52	17.43	Coalesced bubble flow

i. *Full of Water:* The air compressor was turned off for the first three cases (as there was no gas flow in the test loop). Only deionised water flows through the column was tested in this condition. In Case 1, only a small amount of water was regulated through the loop in order to establish a low-speed liquid flow. However, for the remaining cases, the amount of water regulated was increased to fill the pipe with liquid and to develop a dynamic flow of deionised water through the test section of the sensor.

ii. *Discrete Bubble Flow:* It predominates at low gas and liquid velocities and can be characterized by small bubbles with relatively uniform size distributions. The bubble size in the discrete bubble flow regime may be influenced by the gas distributor. For Case No. 4 – 6, the compressor was set on and the air was allowed to enter in the sensor with a low flow rate, subsequently the liquid flow rate starts increasing until discrete bubble flow regime appears.

iii. *Dispersed Bubble Flow:* For Case No. 7 - 9, dispersed bubble flow regime is achieved by further increasing the liquid velocities. It can be characterized by small bubbles with relatively uniform size distributions. The bubbles in this regime, however, are smaller and more uniform because of liquid turbulence.

iv. *Coalesced Bubble Flow:* Finally Case No. 10 - 12 was studied. Here, air varied at the maximum flow rate by keeping the water at lower flow rates. This flow regime is confined to a very narrow gas velocity range.

Different kinds of bubble flow regimes were observed by varying the velocities of air and deionised water as mentioned in Table 4.6. The physical observations of these regimes are discussed in detail in Chapter No. 5. This test matrix also helps in generating the bubble flow regime map for air-water two-phase bubble flow. Table 4.7 provides the summary of the ranges of the experimental parameters covered.

Table 4.7: Experimental Ranges Covered

Experimental Parameter	Range Covered
Gas	Air
Liquid	Deionised Water
Air Superficial Velocity (m/s)	0.00218 – 0.0305
Water Superficial Velocity (m/s)	0.00436 - 0.0349
Water Temperature (°C)	20 – 24 °C

4.11.3 Still Images and Videoing

The flow pattern observations were made through clear Perspex section of an ECT sensor during all the experimental runs. A high resolution digital camera cum video was used to record images and video clips for observations and experiments. It uses 230 kilo pixels with 20 x lens (that extends from 28 mm at the wide end all the way to 560 mm at the telephoto end), HD video recording, a large 3” tilting LCD screen, up to 10 frames per second continuous shooting speeds, and special shooting modes. All this built around an all-new CMOS sensor. It required no additional backlight to take photos. It is equipped with 2 GB memory card to store the photographs which could be later transferred to the computer. It was used for videoing at the vertically installed column made of Perspex. The proper lighting was considered for good images; in addition, the camera was installed for video making at a height of 1.17 m above the floor to capture the videos for two-phase flows. Still images also used to deduce the bubble diameter and void fraction.

4.12 Summary

This chapter has presented the details of an air-water two-phase flow experimental rig developed at laboratory scale. The facility is designed to perform investigations of hydrodynamic behaviour in 49.3 mm inner diameter vertical ECT sensor (i.e. co-current bubble column). The air and deionised water were used as working fluids in this experimental setup. Section 4.1 contains an introduction of the chapter. In sections 4.2 to 4.9, the details of air and deionised water supply facilities, test section (ECT sensor) along with the metering, instrumentation section and data acquisition system has been presented. The test section is made up of Perspex to observe the flow pattern occurring in vertical column. The signals obtained from the data acquisition system are analysed using the ECT software.

In section 4.10 the operating conditions were defined to perform the experiments. Lastly, in section 4.11 the methodology adopted to perform experiments were discussed in detail; test matrix was generated to define the bubble flow regime map, void fraction determination by differential pressure measurements was also discussed and finally the photographic technique was briefly discussed to work out the bubble parameters and the void fraction.